Analysis of integral and averaged characteristics of the IMB and Kamioka signals from SN1987A

A. MAL′GIN
Institute for Nuclear Research of the Russian Academy of Sciences
60th October Anniversary Prospect 7a, Moscow, 117312, Russia

(ricevuto il 22 Settembre 1997; approvato il 20 Ottobre 1997)

Summary. — The shape of angular and temporal integral distributions and averaged characteristics of the IMB and Kamioka events have been discussed. The analysis has shown that the IMB and Kamioka angular distributions of the events in the forward hemisphere ($7+7$ events) are consistent with each other and with the hypothesis of νe-scattering provided that some justified transformation of IMB angles was performed. The temporal distribution of events can be described by an exponential law $\exp[-t/\tau]$ with $\tau \simeq 2.1$ s in the range from 0 to ~ 2.7 s.

PACS 98.52 – Normal galaxies; extragalactic objects and systems (by type).
PACS 96.40 – Cosmic rays.

1. – Introduction

The analysis of the IMB and Kamioka data (tables I, II [1, 2]) presented below is founded on the following three principles:

i) the experimental data are available by itself without looking at a star collapse theory;

ii) the integral and averaged characteristics of the recorded signals only are significant;

iii) both IMB and Kamioka signals are produced by the neutrino flux from SN 1987A.

The first principle determines the types of characteristics which are selected for analysis, namely, the angular and temporal ones. They carry information about composition and temporal behaviour of the neutrino flux, whereas energy characteristics can be informative only when some theoretic assumptions about a spectrum of neutrinos from a collapsing star are accepted.

The second principle seems natural given the poor statistics available and rather large experimental errors. It was used repeatedly in discussions of the data under

TABLE I. – IMB *data* [1]. *Target mass* 6800 ton; $t(0) = 7{:}35{:}41,37$ UT.

No.	$t(s)$	E(MeV)	Θ(deg)	Θ^*(deg)	$\cos\Theta$	$\sin\Theta$	$p_\parallel = E\cdot\cos\Theta$	$p_\perp = E\cdot\sin\Theta$
1	0	38 ± 7	80 ± 10	10	0.17	0.98	6.60	37.42
2	0.42	37 ± 7	44 ± 15	46	0.72	0.69	26.61	25.53
3	0.65	28 ± 6	56 ± 20	34	0.56	0.83	15.66	23.21
4	1.15	39 ± 7	65 ± 20	25	0.42	0.91	16.48	35.35
5	1.57	36 ± 9	33 ± 15	57	0.84	0.54	30.19	19.61
6	2.69	36 ± 6	52 ± 10	38	0.61	0.79	22.16	28.37
7	5.01	19 ± 5	42 ± 20	48	0.74	0.67	14.12	12.71
8	5.59	22 ± 5	104 ± 20	—	—	—	—	—
Mean of seven events		$\langle E\rangle$ 33.3	$\langle\Theta\rangle$ 53.1 ± 6.1	$\langle\Theta^*\rangle$ 36.8 ± 6.1	$\langle\cos\Theta\rangle$ 0.58	$\langle\sin\Theta\rangle$ 0.77	$\langle p_\parallel\rangle$ 18.83	$\langle p_\perp\rangle$ 26.02
				$\Theta^* = 90^\circ - \Theta$; $\cos\Theta^* = \sin\Theta$				

TABLE II. – *Kamioka data* [2]. *Target mass* 2140 ton.

No.	$t(s)$	E(MeV)	Θ(deg)	$\cos\Theta$	$\sin\Theta$	$p_\parallel = E\cdot\cos\Theta$	$p_\perp = E\cdot\sin\Theta$
1	0	20 ± 2.9	18 ± 18	0.95	0.31	19.02	6.18
2	0.107	13.5 ± 3.2	40 ± 27	0.77	0.64	10.34	8.68
3	0.303	7.5 ± 2.0	108 ± 32	—	—	—	—
4	0.324	9.2 ± 2.7	70 ± 30	0.34	0.94	3.15	8.64
5	0.507	12.8 ± 2.9	135 ± 23	—	—	—	—
6	1.541	35.4 ± 8.0	32 ± 16	0.85	0.53	30.02	18.76
7	1.728	21.0 ± 4.2	30 ± 18	0.87	0.50	18.19	10.05
8	1.915	19.8 ± 3.2	38 ± 22	0.79	0.61	15.60	12.19
9	9.219	8.6 ± 2.7	122 ± 30	—	—	—	—
10	10.433	13.0 ± 2.6	49 ± 26	0.66	0.75	8.53	9.81
11	12.439	8.9 ± 1.9	91 ± 39	—	—	—	—
Mean of seven events		$\langle E\rangle$ 18.8	$\langle\Theta\rangle$ 39.6 ± 8.7	$\langle\cos\Theta\rangle$ 0.75	$\langle\sin\Theta\rangle$ 0.61	$\langle p_\parallel\rangle$ 14.98	$\langle p_\perp\rangle$ 10.61

consideration. In the present analysis an integral distribution (spectrum) shape is selected as the integral characteristics. It is commonly known that integral spectrum points represent the intensity of events at a given argument value and, therefore, they are interconnected. For this reason an integral spectrum is of a more smooth form in comparison with a differential one and reflects the main features of the data set to be analysed. This circumstance is of particular assistance in the low-statistics case.

2. – Angular characteristics

A shape of integral distribution of the events over the angle Θ and the average value $\langle\Theta\rangle$ were selected as angular characteristics. Θ is an angle between an electron track and the neutrino direction. Distribution over the azimuthal angle φ was not

considered since it cannot provide any information of the neutrino flux with the accepted experimental procedure and with an assumption that it was SN 1987A that generated the neutrinos.

The angular analisys consists in the comparison between the selected characteristics of the IMB and Kamioka signals and with expectations. Both the isotropic distribution and the angular distribution of recoil electrons due to the $\nu e \to \nu' e'$ reaction are used in calculations of the expected characteristics. The isotropic distribution corresponds to the $\bar{\nu}_e p \to n e^+$ reaction in the energy range from 10 to 50 MeV. The role of the $^{16}O(\nu_e, e^-)^{16}F$ reaction in the shaping of a spatial distribution of the IMB and Kamioka events will be discussed later.

The differential angular distribution of positrons from the $\bar{\nu}_e p$-reaction (fig. 1a)) can be described by the following expression:

$$\frac{dN}{d\Theta} = \text{const} \cdot \sin\Theta \,. \tag{1}$$

The isotropic distribution takes suck a form due to solid-angle effect by virtue of which the distribution is symmetric and has the maximum at $\Theta = 90°$. These peculiarities determine the average angle value of $\overline{\Theta}_{\text{isotr}} = 90°(0 \leqslant \Theta \leqslant 180°)$.

The spatial distribution of recoil electrons from the $\nu e \to \nu' e'$ reaction can be expressed in the following way [3]:

$$\frac{dN}{d\Theta} = \sin\Theta \cdot \exp\left[\frac{\Theta^2}{2\sigma^2}\right]. \tag{2}$$

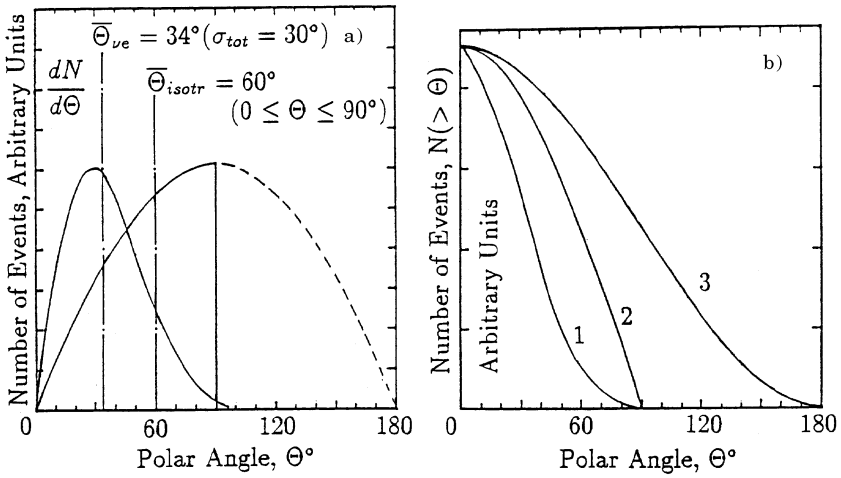

Fig. 1. – a) The differential angular spectra. The left solid curve corresponds to νe-scattering. The right solid curve corresponds to the isotropic distribution in the forward hemisphere. The dashed curve represents the isotropic distribution in the backward hemisphere. b) The integral angular spectra: 1: νe-scattering; 2: the isotropic distribution in the forward hemisphere ($0 \leqslant \Theta \leqslant 90°$); 3: the total isotropic distribution ($0 \leqslant \Theta \leqslant 180°$). The spectra are normalized to the same number of events.

This formula is approximate because a $\Theta(E)$-dependence is not involved. But it is reasonably accurate since the recoil electron deflects from a neutrino direction just after collision no more than by 5° within the energy range from 10 to 50 MeV under consideration. A further increasing in angle value (up to the mean angle value of $\sim 24°$) is due to multiple-electron scattering in water. This is the process that forms a Gaussian shape of the final distribution.

The sin Θ factor accounts for the solid-angle effect. The σ parameter characterizes the total deflection of reconstructed track from the neutrino flux direction and, hence, its magnitude depends on both multiple-electron scattering and track reconstruction error:

$$\sigma_{\text{tot}} = \sqrt{\sigma_{\text{sc}}^2 + \sigma_{\text{rec}}^2}\,. \tag{3}$$

The σ_{sc} value corresponding to the mean angle of 24° is equal to 20°. The errors of track reconstruction for IMB and Kamioka experiments are somewhat different:

$$\langle \sigma_{\text{rec}}^{\text{IMB}} \rangle \simeq 16.2°\,, \qquad \langle \sigma_{\text{rec}}^{\text{Kam}} \rangle \simeq 25.5° \qquad \text{(tables I, II)}\,.$$

Assuming that the reconstruction errors for both experimets are approximately the same ($\langle \sigma_{\text{rec}} \rangle = 20°$), we obtain

$$\sigma_{\text{tot}} = \sqrt{\sigma_{\text{sc}}^2 + \sigma_{\text{rec}}^2} \simeq 28°\,.$$

More precisely, $\langle \sigma_{\text{tot}}^{\text{IMB}} \rangle = 25.7°$, $\langle \sigma_{\text{tot}}^{\text{Kam}} \rangle = 32.4°$. Obviously, the $\overline{\Theta}_{\nu\text{e}}$ value depends on σ_{tot}. In fig. 1a), b) both the differential and integral angular spectra are shown. The νe-scattering spectrum was calculated at $\sigma_{\text{tot}} = 30°$.

Figure 2 presents the integral distributions of the IMB and Kamioka events. The computed spectra are normalized to the total amount of events. As can be seen from fig. 2, the combined experimental distribution agrees neither in shape, nor in value $\langle \Theta \rangle$ with neither of the two calculated spectra. The average angle $\langle \Theta \rangle = 63.6° \pm 5.2°$ of the combined IMB + Kamioka sample differs from the expected value $\overline{\Theta}_{\text{isotr}} = 90°$ by more than 5 standard deviations. At the same time, it can be noted that the combined IMB and Kamioka distribution follows to the νe-spectrum calculated at $\sigma_{\text{tot}} = 30°$ in the angular range from about 25° to 55°.

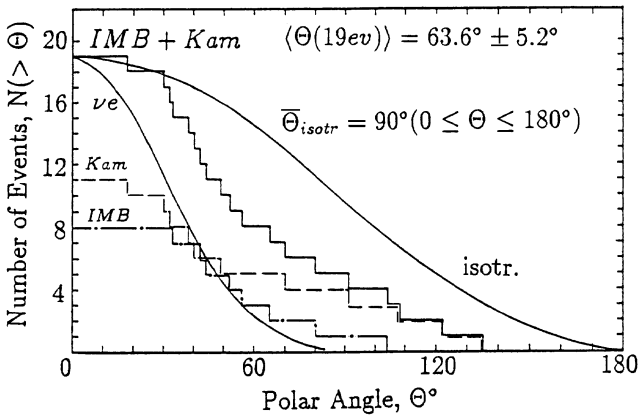

Fig. 2. – The integral angular distributions of the IMB and Kamioka events. The histograms represent the experimental data. The curves are expected spectra.

A noticeable anisotropy of both signals has been brought to the attention immediately after the publication of the experimental data [4, 5]. The angular anisotropy of the IMB signal is accepted by authors of the IMB experiment [1, 3, 6]. Spatial directivity of the signal seems puzzling to the authors even with due regard to the fact that 25% of the detector PMTs were not operating at the moment of the neutrino burst [1].

As the data of tables I, II suggest, seven events of either of the two signals are in the forward hemisphere $0 \leqslant \Theta \leqslant 90°$. Thus, about 75% of the total amount of the events (19 events) belong to the forward hemisphere. Those 14 events are considered below. When discussing the forward-directed events (fw-events), one must take into account that in the case of isotropically directed tracks an angular distribution for the forward hemisphere has a truncated form in comparison with the total distribution in the angular range from 0 to 180° (fig. 1a), b)). Hence, the mean angle $\overline{\Theta}_{\text{isotr}}$ is to be equal to 60° in the angle interval from 0 to 90°.

The integral angular distribution of the Kamioka fw-events is presented in fig. 3. It agrees more than satisfactorily with the expected spectrum for νe-scattering at $\sigma_{\text{tot}} = 30°$. This fact can be expressed by the relation

$$N(> \Theta_{\text{Kam}}) \simeq N(> \Theta_{\nu e}) \tag{4}$$

at $\Theta_{\text{Kam}} = \Theta_{\nu e}$ and $\sigma_{\text{tot}} = 30°$.

The value $\sigma_{\text{tot}} = 30°$ is used in the following calculations, since it is approximately equal to the average for both experiments. This value determines the mean angle of the expected angular distribution of recoil electron reconstructed tracks $\overline{\Theta}_{\nu e} = 34°$ (fig. 1a)).

The average angle of the Kamioka fw-events is $\langle \Theta_{\text{Kam}} \rangle = 39.6° \pm 8.7°$ which agrees with $\overline{\Theta}_{\nu e} = 34°$ within the limits of one standard deviation. At the same time, the $\langle \Theta_{\text{Kam}} \rangle$ value differs by more than two standard deviations from the value $\overline{\Theta}_{\text{isotr}} = 60°$.

So, the analysis of both the angular-distribution shape and the value of the average angle gives grounds to conclude that the Kamioka fw-events can be associated with νe-scattering.

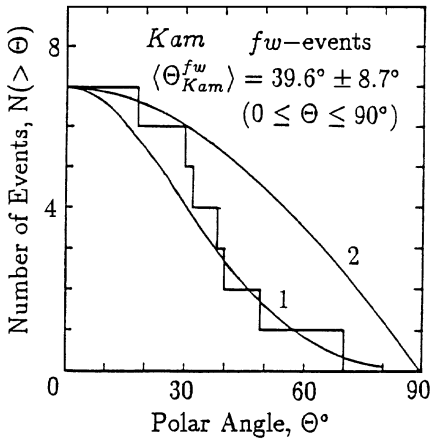

Fig. 3. – The integral angular Kamioka distributions. The histogram represents the fw-events; curve 1 is the calculated νe-scattering spectrum at $\sigma_{\text{tot}} = 30°$; curve 2 is the isotropic distribution in the forward hemisphere.

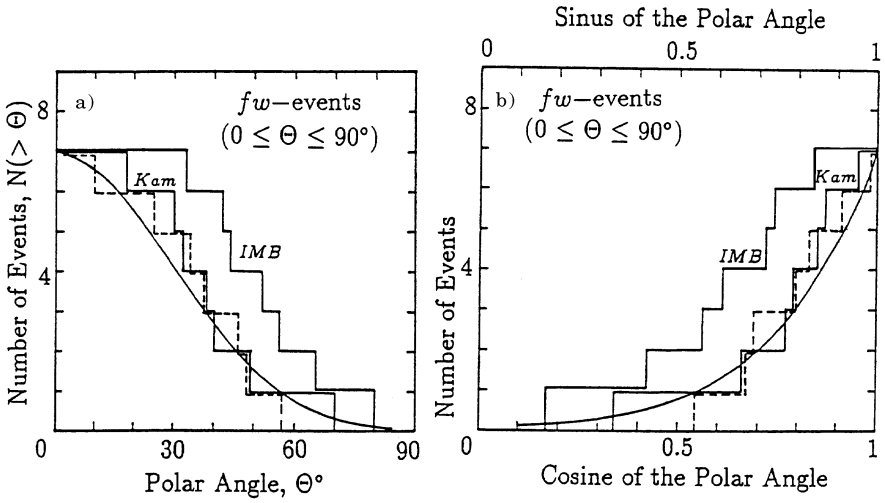

Fig. 4. – *a*) The integral angular distributions of the fw-events. The solid-line histograms are experimental data; the dashed line represents the transformed IMB(Θ^*) data. The solid curve is the expected νe-scattering spectrum at $\sigma_{\text{tot}} = 30°$. *b*) The cumulative angular distributions of the fw-events. The solid-line histograms are distributions over $\cos\Theta$. The dashed-line histogram is a distribution of the IMB events over $\sin\Theta$. The solid curve is the expected νe-scattering spectrum at $\sigma_{\text{tot}} = 30°$.

The average angle of the IMB fw-events is $\langle\Theta_{\text{IMB}}\rangle = 53.1° \pm 6.1°$. This magnitude is close to the mean angle of the isotropic spectrum: $\overline{\Theta}_{\text{isotr}} = 60°$ ($0 \leqslant \Theta \leqslant 90°$). However, there are two more peculiarities of the IMB data: firstly, the fw-events distributions (fig. 4a), b)) being shifted to greater angles are identical to the Kamioka fw-event distributions and, secondly, the $N(<\sin\Theta)$ distribution is almost superposing on the $N(<\cos\Theta)$ Kamioka distribution (fig. 4b)).

A calculated cumulative $N(<\cos\Theta)$ spectrum was obtained using the differential angular spectrum of scattered electrons in the form

$$\frac{\mathrm{d}N}{\mathrm{d}(\cos\Theta)} = \exp\left[-\frac{\Theta^2}{2\sigma^2}\right], \tag{5}$$

here σ has the same meaning as in the expression (2).

The superposition of the $N(<\sin\Theta)$ IMB and $N(<\cos\Theta)$ Kamioka distributions on one another can be expressed in the following way:

$$N(<\sin\Theta_{\text{IMB}}) \simeq N(<\cos\Theta_{\text{Kam}}) \tag{6}$$

at

$$\sin\Theta_{\text{IMB}} = \cos\Theta_{\text{Kam}}\,. \tag{7}$$

And since $\cos\Theta_{\text{Kam}} = \cos\Theta_{\nu e}$, then $\sin\Theta_{\text{IMB}} = \cos\Theta_{\nu e}$.

Hence, it follows that

$$\Theta_{\text{IMB}} = 90° - \Theta_{\nu e}\,. \tag{8}$$

So, in the IMB experiment the angle Θ_{IMB} may have been determined instead of the actual angle $\Theta^* = 90^\circ - \Theta_{\mathrm{IMB}} (\Theta^* = \Theta_{\nu e})$.

Really,

$$\sin \Theta_{\mathrm{IMB}} = \sin (90^\circ - \Theta^*_{\mathrm{IMB}}) = \cos \Theta^*_{\mathrm{IMB}} \tag{9}$$

and the distribution over $\sin \Theta_{\mathrm{IMB}}$ corresponds to a distribution over $\cos \Theta^*$ (fig. 4b)). This could occur due to confusion of trigonometric functions, something like $\sin \Theta \leftrightarrow \cos \Theta$ or $\arcsin X \leftrightarrow \arccos X$ in the track reconstruction program for the SN1987A events. The transformation of the IMB angles $\Theta_{\mathrm{IMB}} \rightarrow \Theta^*$ within the angular interval $0 \leqslant \Theta \leqslant 90^\circ$ leads to replacement of small angles with large ones and *vice versa* (table I), while the angles near $\Theta = 45^\circ$ are changed slightly. The only event No. 8 in the backward hemisphere takes the magnitude

$$\Theta^*(\mathrm{No.\ 8}) = 90^\circ - 104^\circ = -14^\circ ,$$

which can be interpreted as $\Theta^*(\mathrm{No.\ 8}) = 180^\circ - 14^\circ = 166^\circ$.

The transformed distribution of IMB fw-events is shown in fig. 4a). As can be seen, the IMB (Θ^*) distribution is almost superposed on the Kamioka distribution. Due to the transformation the average IMB angle of the fw-events changes from $53.1^\circ \pm 6.1^\circ$ to $36.9^\circ \pm 6.1^\circ$ which is in agreement both with $\langle \Theta^{\mathrm{fw}}_{\mathrm{Kam}} \rangle = 39.6^\circ \pm 8.7^\circ$ and with $\overline{\Theta}_{\nu e} = 34^\circ$ within the limits of one standard deviation.

It may appear that there is another way to bring the IMB and Kamioka distributions into coincidence, namely, by means of shifting the $N(> \Theta)$ IMB distribution to the Kamioka distribution by $\Theta = 15^\circ$ or, what is the same, by introducing an angle $\Theta^* = \Theta_{\mathrm{IMB}} - 15^\circ$ in the IMB signal analysis. Applying such a shift would signify that each of IMB angles is overestimated by 15°. An appearance of the constant value $\Theta = 15^\circ$ in the track reconstruction program is difficult to explain.

An important feature of the integral $N(> \Theta)$ and $N(< \cos \Theta)$ distributions should be noted, namely, the distribution shape invariance (within the limits of statistics) under the angle transformation. In the case of the $N(> \Theta)$ distribution the invariance is explained by a quasi-symmetric form of the differential νe-spectrum $\mathrm{d}N/\mathrm{d}\Theta$ (fig. 1); for the $N(< \cos \Theta)$ distribution it is determined by properties of the differential spectrum $\mathrm{d}N/\mathrm{d}(\cos \Theta)$.

One can consider another average characteristic of the fw-events like an anisotropy parameter $R(\Theta)$:

$$R(\Theta) = \frac{\langle p_{\parallel} \rangle}{\langle p_{\perp} \rangle} = \frac{\langle E \cos \Theta \rangle}{\langle E \sin \Theta \rangle} ; \tag{10}$$

here $\langle p_{\parallel} \rangle$ and $\langle p_{\perp} \rangle$ are mean values of longitudinal and transversal momentum components, respectively:

$$\langle E \cos \Theta \rangle = \frac{\sum_{i=1}^{N} E_i \cos \Theta_i}{N} , \qquad \langle E \sin \Theta \rangle = \frac{\sum_{i=1}^{N} E_i \sin \Theta_i}{N} , \qquad N = 7 .$$

In more exact terms, R should be determined as a testing parameter to examine a spatial track distribution for isotropy. It was precisely the sense in which the R parameter has been applied in the present analysis since a hypothesis is commonly adopted that the IMB and Kamioka events are caused mainly by positrons from the

$\overline{\nu}_e p \to e^+ n$ reaction and therefore their tracks are isotropic. Obviously, for an isotropic angular distribution at high statistics $R \to 1$.

For the Kamioka fw-events $R_{\text{Kam}} = 1.41$, for the IMB fw-events $R_{\text{IMB}} = 0.72$ (table I, II). Due to transformation $\Theta_{\text{IMB}} \to \Theta^*$ we get the value

$$R(\Theta^*) = \frac{\langle E \cos \Theta^* \rangle}{\langle E \sin \Theta^* \rangle} = \frac{\langle E \sin \Theta \rangle}{\langle E \cos \Theta \rangle} = \frac{1}{R(\Theta)} = 1.39$$

which practically coincides with R_{Kam}.

It can be noted that the expected value of the anistropy parameter is approximately $R(\overline{\Theta}_{\nu e}) = \cos 34^\circ / \sin 34^\circ = 1.48$ since Θ slightly depends on E within energy range from 10 to 50 MeV.

So, summarizing all the foregoing, one can made the following conclusions:

i) the angular distribution shape of the Kamioka fw-events (7 out of 11), the average angle and the anisotropy parameter correspond to νe-scattering, taking into account that the total error in determining the neutrino direction σ_{tot}, conditioned by the experimental procedure, is 30°;

ii) the angular distribution shape of the IMB fw-events (7 out of 8 events) is consistent with νe-scattering at $\sigma_{\text{tot}} = 30^\circ$;

iii) having transformed the IMB angles as follows: $\Theta_{\text{IMB}} \to \Theta^* = 90^\circ - \Theta_{\text{IMB}}$, we can see that the angular distribution of the IMB fw-events as well as the $\langle \Theta^* \rangle$ and $R(\Theta^*)$ values are consistent with νe-scattering.

These conclusions remain valid with use of the initial IMB and Kamioka data [7, 8].

3. – Discussion

Assuming that the peculiarities i)-iii) of the experimental data are not connected with νe-scattering, we have to attribute them to statistic fluctuations and, therefore, we are dealing with at least threefold accidental coincidence. When these facts are considered to be associated with νe-scattering, it must be supposed that there is a mistake in the IMB reconstruction program.

When estimating a personal probability of the two options, one can say that an appearance of the confusion of a kind of $\sin \Theta \leftrightarrow \cos \Theta$ or $\arccos X \leftrightarrow \arcsin X$ in the track reconstruction program is quite possible the more so that it is overcrowded with trigonometric functions. At the same time, it seems less probable that the agreement of the angular characteristics of the IMB and Kamioka signals and their consistency with the νe-scattering obtained after the transformation of the IMB angles are accidental.

Following the νe-scattering hypothesis the combined IMB(Θ^*) and Kamioka angular distribution of the 14 fw-events can be plotted. They are shown in fig. 5a), b). The distribution shapes and the average angle value of $\langle \Theta(14 \text{ fw-events}) \rangle = 38.2^\circ \pm 5.3^\circ$ are statistically backed up and are in good agreement with the appropriate characteristics of νe-scattering.

One would advance in this direction still further. The average energy of the Kamioka fw-events is $\langle E_{\text{Kam}}^{\text{fw}} \rangle = 18.8$ MeV. An energy of a recoil electron is connected with a neutrino energy on the average by the following relation: $\langle E_\nu \rangle \simeq 2 \langle E_e \rangle$.

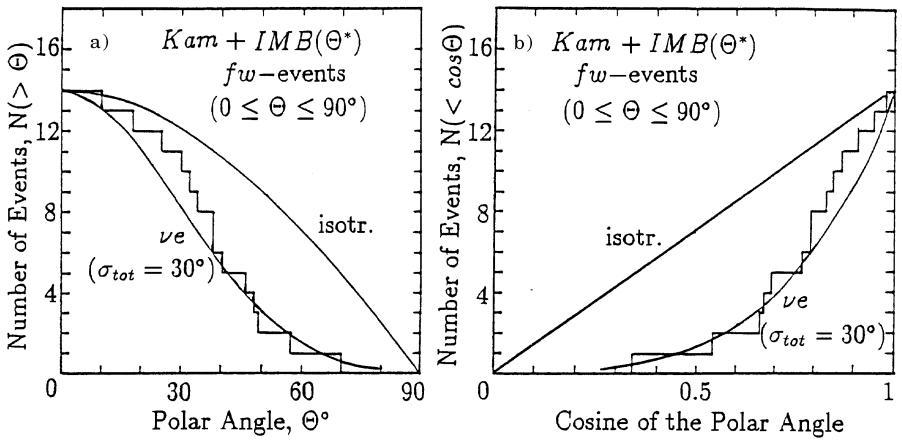

Fig. 5. – *a*) The integral angular distribution of the 14 IMB(Θ*) + Kamioka fw-events. The solid curves are calculated spectra. *b*) The cumulative angular distribution of the 14 IMB(Θ*) + Kamioka fw-events. The solid curves are calculated spectra.

The main contribution to the $\nu e \to \nu' e'$ process is made by electron neutrinos which are of the most νe-scattering cross-section among all kinds of neutrino (approximately 6 times more). Therefore, the energy which can be attributed to the electron neutrino flux, without considering the detector trigger efficiency, is

$$\langle E_\nu \rangle \simeq 2\langle E_e \rangle = 2 \cdot 18.8 \text{ MeV} \simeq 38 \text{ MeV} .$$

At such a high energy the role of the $^{16}O(\nu_e, e^-)^{16}F$ reaction becomes significant. The reaction has the energy threshold about 13 MeV:

$$\sigma(\nu_e {}^{16}O) \simeq 1.1[E_\nu(\text{MeV}) - 13]^2 \cdot 10^{-44} \text{ cm}^2 \text{ [9]} .$$

The electron kinetic energy is related to the neutrino energy in the following way:

$$E_e \simeq E_\nu - 13 \text{ MeV} .$$

Electrons are mainly directed in the backward hemisphere [10].

The average energy of the four Kamioka backward events is less by 9.4 MeV than the average energy of the seven fw-events: 9.4 and 18.8 MeV, respectively. This fact gives grounds to associate the backward events for the most with the $^{16}O(\nu_e, e^-)^{16}F$ reaction.

Figure 6 shows the calculated angular spectra of the reconstructed electron tracks from both the $\nu e \to \nu' e'$ and $^{16}O(\nu_e, e^-)^{16}F$ reactions at $\sigma_{tot} = 30°$.

The $^{16}O(\nu_e, e^-)^{16}F$ angular distribution is obtained on the basis of paper [10]. As can be seen from the graphs, a fairly large part of the $^{16}O(\nu_e, e^-)^{16}F$ distribution is placed in the forward hemisphere (about 40%). Consequently, the $\nu e \to \nu' e'$ and $^{16}O(\nu_e, e^-)^{16}F$ distributions overlap.

Because of this, the fw-events having the largest angles, namely, Kamioka event No. 4 and IMB event No. 5 can be associated both with νe-scattering and with $\nu_e {}^{16}O$ charged-current nuclear scattering. Therefore, 6 events of either signal could be

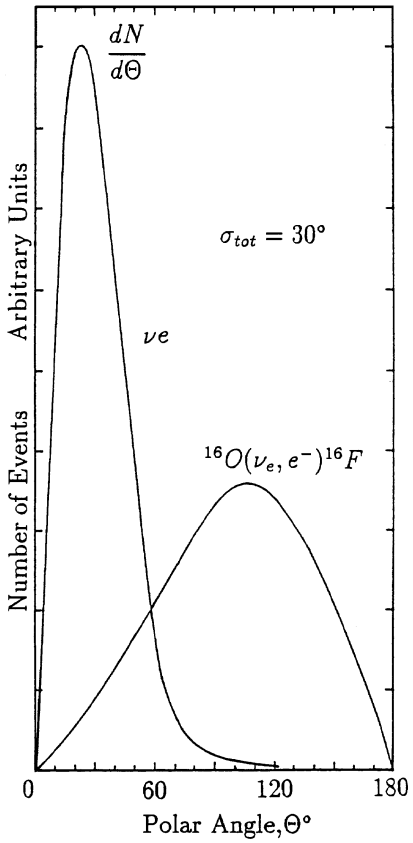

Fig. 6. – The calculated differential angular spectra. The spectra are normalized to the same number of events.

assigned with confidence to νe-scattering and the remaining events to the $^{16}O(\nu_e, e^-)^{16}F$ reaction.

The foregoing signifies that the hypothesis under consideration eliminates the presence of a noticeable component of $\overline{\nu}_e$ p-interactions in the IMB and Kamioka signals.

Both high energy of the neutrinos and the absence of $\overline{\nu}_e$-component could point to the fact that the SN1987A neutrino flux recorded by IMB and Kamioka has the origin different from the initial core collapse to a neutron star.

Judging by the experimental data, their angular and energy features only, the more suitable candidate among "natural" neutrino sources is π^+-decay at rest. As a result, three types of neutrinos are produced: monoenergetic ν_μ with $E_{\nu_\mu} = 29.8$ MeV and ν_e and $\overline{\nu}_\mu$ with energies up to 52.8 MeV. For ν_e and $\overline{\nu}_\mu$ the effective energies are about 37 MeV and 43 MeV, respectively, when the dependence of the cross-section $\sigma(\nu e)$ on energy is taken into account.

Given the number of the recorded νe-interactions, one can estimate the total neutrino flux. To do this, the energy spectra, the detection efficiency, the detector's

energy resolution and a distance from the neutrino source of $1.5 \cdot 10^{23}$ cm must be taken into consideration.

As a result, the ν_e-flux is $\Phi_{\nu_e} = 2.2 \cdot 10^{10}\ \mathrm{cm}^{-2}$ and the total neutrino flux is $\Phi_\nu = 3\,\Phi_{\nu_e} = 6.6 \cdot 10^{10}\ \mathrm{cm}^{-2}$. This value corresponds to the total amount of decaying pions of about $6.4 \cdot 10^{57}$ and the total energy of $1.0 \cdot 10^{54}$ erg which is carried out in the neutrino pulse.

4. – Integral temporal distributions

In some papers efforts were made to analyse a bunch structure of the SN1987A event temporal distributions [11, 12]. The resulting conclusions have been bearing a debating nature since the authors had to deal, in fact, with differential distributions. In the case of poor statistics available, the identification of a differential distribution shape is extremly complicated. As a consequence, differential temporal distributions of the SN1987A events can be associated with a variety of hypothesis.

Figure 7 shows the integral temporal distribution of the IMB events in a semilog scale. As indicated in the figure, the distribution can be described reasonably well by a straight line within the range from 0 to 3 s.

It is evident that integral and differential forms of the exponential law are identical. Hence, we can state an impressive agreement of the IMB temporal distribution with the exponential law within the range from 0 to 3 s:

$$\Phi_\nu(t) = \Phi_0 \exp\left[-\frac{t}{\tau}\right], \qquad \tau \simeq 2.1\ \mathrm{s}\,.$$

In fig. 7 the teoretical integral spectrum is also shown to give an idea about results of calculations of a $\bar{\nu}_e$ flux temporal dependence $L_{\bar{\nu}_e}(t)$. The integral spectrum was derived from a differential one which was obtained in paper [13].

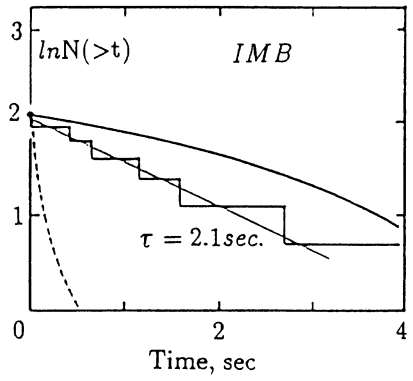

Fig. 7. – The integral temporal distribution of the IMB events. The straight line corresponds to the exponential law with $\tau = 2.1$ s; the dashed curve corresponds to the calculations [13]; the solid curve is calculated for the events uniformly distributed within the interval from 0 to 5.6 s (IMB signal duration).

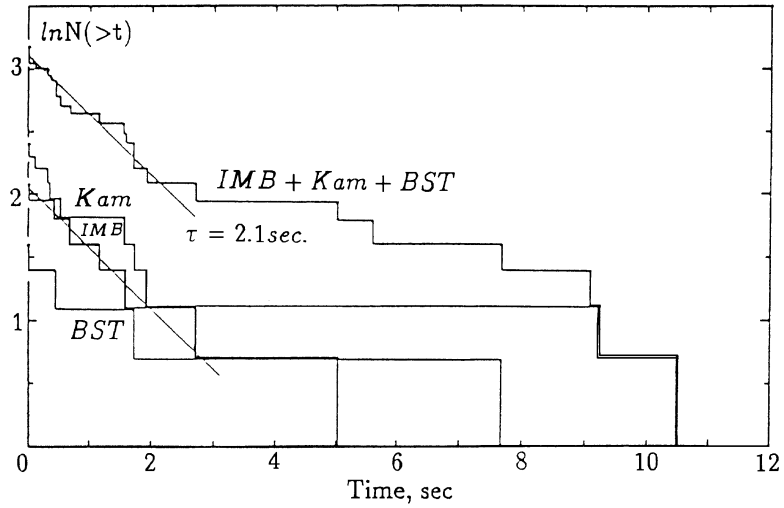

Fig. 8. – The integral temporal distributions. The straight lines represent the exponential law with $\tau = 2.1$ s. The time $t = 0$ corresponds to the first event of each signal.

Temporal dynamics of the ν flux have been considered in the literature [14] in some details. The author has concluded that a two-exponent curve gave the best fit to the calculated $L_\nu(t)$-dependence: an exponent with $\tau < 1$ s should be of better use during the first two seconds and the exponent with $\tau \sim 4$ s at $t > 2$ s. In addition, it was obtained that the temporal structure of the Kamioka signal agreed with some of the models which have been considered, whereas the IMB signal is consistent with none of them.

Figure 8 presents temporal distributions of all signals which have been recorded at the time 7:35 UT including BST data (table III [15]).

It can be seen that each of the distributions does not contradict to the τ value of 2.1 s which was determined on the basis of IMB data. The similarity of the distributions favours the view that they are connected with the same neutrino flux. The combined distribution ($N_{\text{tot}} = 24$ events) agrees well with the exponential law with $\tau = 2.1 \pm 0.2$ s within the time interval $0 \leqslant t < 2.7$ s. From the combined distribution one can conclude that at $t \geqslant 2.7$ s (7 events) an exponent increases or the temporal distribution takes a different (nonexponential) shape.

Following the accepted approach, *i.e.* analyzing the integral and average characteristics, let us introduce an average time interval Δt between the events in the

TABLE III. – BST *data*.

Relative time	Energy (MeV)	Internal or external
0.000	12.0 ± 2.4	internal
0.435	18.0 ± 3.6	internal
1.710	23.3 ± 4.7	external
7.687	17.0 ± 3.4	external
9.099	20.1 ± 4.0	external

range $0 \leqslant t < 2.7$ s. The calculated $\overline{\Delta t}$ value is

$$\overline{\Delta t} = \frac{t^*}{N_{\text{tot}}[1 - \exp[-t^*/\tau]] - 1} \; ; \tag{11}$$

here $\tau = 2.1$ s, N_{tot} is a total number of events in a signal.

The time t^* sets the temporal interval within which the $\overline{\Delta t}$ value is determined: $t^*_{\text{IMB}} = 2.69$ s (event No. 6), $t^*_{\text{Kam}} = 1.915$ s (event No. 8), $t^*_{\text{BST}} = 1.71$ s (event No. 3), $t^*_{\text{C}} = 2.69$ s. The calculated $\overline{\Delta t}$ values are as follows:

$$\overline{\Delta t}_{\text{IMB}} = 0.56 \text{ s}\,, \quad \overline{\Delta t}_{\text{Kam}} = 0.34 \text{ s}\,, \quad \overline{\Delta t}_{\text{BST}} = 0.96 \text{ s}\,, \quad \overline{\Delta t}_{\text{C}} = 0.16 \text{ s}\,.$$

The experimental values are:

$$\overline{\Delta t}_{\text{IMB}} = 0.54 \text{ s}\,, \quad \overline{\Delta t}_{\text{Kam}} = 0.27 \text{ s}\,, \quad \overline{\Delta t}_{\text{BST}} = 0.85 \text{ s}\,, \quad \overline{\Delta t}_{\text{C}} = 0.17 \text{ s}\,.$$

So, the $\overline{\Delta t}$ value also indicates good agreement of the temporal behaviour of the SN1987A signals at the initial stage with the exponent $\tau = 2.1$ s, especially in the combined distribution case.

* * *

I would like to thank G. T. ZATSEPIN for benevolent reading of the manuscript. I am grateful to my colleagues V. FULGIONE, S. P. MIKHEYEV, O. G. RYAZHSKAYA, V. G. RYASNY and O. SAAVEDRA for interest to this work and useful discussions.

REFERENCES

[1] BRATTON C. B. *et al.*, *Phys. Rev. D*, **37** (1988) 3361.
[2] HIRATA K. *et al.*, *Phys. Rev. D*, **38** (1988) 448.
[3] KIELCZEWSKA D., *Phys. Rev. D*, **41** (1990) 2967.
[4] RYAZHSKAYA O. G. and RYASNY V. G., *Proceedings of the Second International Symposium UP-87, Baksan, USSR 1987* (Nauka, Moskow) 1988, p. 103.
[5] LO SECCO J. M., *Proceedings of the Second International Symposium UP-87, Baksan, USSR 1987* (Nauka, Moskow) 1988, p. 100.
[6] LO SECCO J. M., *Phys. Rev. D*, **39** (1989) 1013.
[7] HIRATA K. *et al.*, *Phys. Rev. Lett.*, **58** (1987) 1490.
[8] BIONTA R. *et al.*, *Phys. Rev. Lett.*, **58** (1987) 1494.
[9] ARAFUNE J. and FUKUGITA M., *Phys. Rev. Lett.*, **59** (1987) 367.
[10] DONNELLY T. W., *Phys. Lett. B*, **43** (1973) 93.
[11] ALEXEYEV E. N., ALEXEYEVA L. N., KRIVOSHEINA I. V. and VOICHENKO V. I., *Proceedings of the Second International Symposium UP-87, Baksan, USSR 1987* (Nauka, Moskow) 1988, p. 85.
[12] SUZUKI H. and SATO K., *Progr. Theor. Phys.* (*Progress Lett.*), **79** (1988) 725.
[13] BRUENN S. W., *Phys. Rev. Lett.*, **59** (1987) 938.
[14] BURROWS A., *Proceedings of the 13th International Conference Neutrino-88, Boston, 1988* (World Scientific, Singapore) 1989, p. 142.
[15] ALEXEYEV E. N. *et al.*, *Pis'ma Zh. Éksp. Teor. Fiz.*, **45** (1987) 461 (*JETP Lett.*, **45** (1987) 589).